BIOCHEMISTRY
including biophysical chemistry & molecular biology

Article

pubs.acs.org/biochemistry

Investigating *Deinococcus radiodurans* RecA Protein Filament Formation on Double-Stranded DNA by a Real-Time Single-Molecule Approach

Hsin-Fang Hsu,[†] Khanh V. Ngo,[‡] Sindhu Chitteni-Pattu,[‡] Michael M. Cox,[‡] and Hung-Wen Li*[,†]

[†]Department of Chemistry, National Taiwan University, Taiwan

[‡]Department of Biochemistry, University of Wisconsin, Madison, Wisconsin 53706, United States

Supporting Information

ABSTRACT: With the aid of an efficient, precise, and almost error-free DNA repair system, *Deinococcus radiodurans* can survive hundreds of double-strand breaks inflicted by high doses of irradiation or desiccation. RecA of *D. radiodurans* (DrRecA) plays a central role both in the early phase of repair by an extended synthesis-dependent strand annealing process and in the later more general homologous recombination phase. Both roles likely require DrRecA filament formation on duplex DNA. We have developed single-molecule tethered particle motion experiments to study the assembly dynamics of RecA proteins on individual duplex DNA molecules by observing changes in DNA tether length resulting from RecA binding. We demonstrate that DrRecA nucleation on double-stranded DNA is much faster than that of *Escherichia coli* RecA protein (EcRecA), but the extension is slower. This combination of attributes would tend to increase the number and decrease the length of DrRecA filaments relative to those of EcRecA, a feature that may reflect the requirement to repair hundreds of genomic double-strand breaks concurrently in irradiated *Deinococcus* cells.

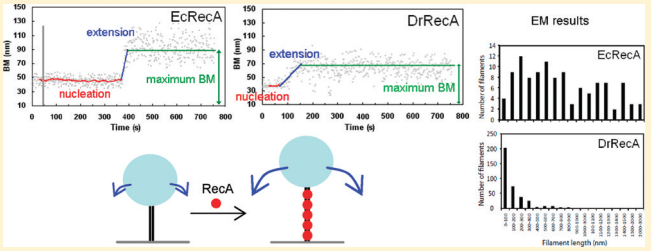

Deinococcus radiodurans is a bacterium that can survive extraordinary doses of ionizing radiation.[1] DNA damage inflicted by ionizing radiation, even when it includes hundreds of double-strand breaks, is repaired within a few hours. The extreme radioresistance appears to be an adaptation to frequent desiccation.[1,2] Double-strand breaks accumulate during dehydration, and radiation-sensitive mutants of *D. radiodurans* are also sensitive to desiccation.[2]

Many hypotheses have been proposed to explain the high-efficiency repair, including a ringlike condensed chromosome structure that could restrict fragment DNA diffusion,[3−5] a high Mn^{2+} concentration that can scavenge hydroxyl radicals,[6] an enhanced capacity for replication fork repair,[7] and the presence of multiple genome copies to facilitate recombinational DNA repair.[3,8] Mechanisms that reduce the level of protein oxidation have emerged as major contributors to extreme radiation resistance, with possible contributions from novel adaptations of DNA repair systems.[9,10]

Repair of the *D. radiodurans* genome after irradiation is strikingly robust, and its mechanism has been studied for decades.[1,11−15] Zahradka et al.[14] proposed that *D. radiodurans* uses overlapping homologies as both primer and template for DNA polymerase to elongate single-strand overhangs, which allows the fragments to anneal to form double strands with high precision. This early phase of extended synthesis-dependent strand annealing (ESDSA) assembles the fragments into much larger chromosomal segments. In a second phase, the double-strand DNA segment is then collected into intact circular chromosomes by homologous recombination mediated by RecA.[13,14]

The bacterial RecA protein plays an essential role in recombination and repair pathways.[7,16−19] RecA is found in all bacteria except a few endosymbiotic *Buchnera* species with smaller genomes.[20] Formation of a RecA nucleoprotein filament is a prerequisite for RecA function and occurs in two steps.[16,21,22] The first step is nucleation. This is then followed by a unidirectional filament extension that proceeds from 5′ to 3′ on single-stranded DNA (ssDNA). For the well-studied *Escherichia coli* RecA (EcRecA), the nucleation step is normally rate-limiting,[21] in which a RecA oligomer consisting of approximately six RecA subunits binds to DNA. When individual RecA molecules assemble on DNA, the DNA is stretched and underwound to form a nucleoprotein filament with its rigidity and end-to-end length increased.[23]

RecA promotes recombination in a wide range of physiological contexts, depending on the lifestyle of a given bacterial species.[1] Reactions can include the repair of stalled replication forks,[17,24−27] conjugational recombination,[28] reactions associated with antigenic variation,[29,30] and genome reconstitution after severe irradiation.[1] It has been postulated that RecA protein encoded by a given bacterial species will exhibit properties

Received: March 21, 2011
Revised: August 15, 2011
Published: August 19, 2011

reflecting the dominant DNA repair scenario encountered by that species.[1,16] With respect to DNA repair, *E. coli* and *D. radiodurans* provide examples of widely divergent lifestyles. *E. coli*, a gut bacterium, is normally shielded from environmental radiation, and its RecA protein (EcRecA) must primarily deal with replication fork repair. Estimates of fork repair frequency vary, but the highest reported rates in a laboratory environment are no more than once per cell per generation.[7,17,31] *D. radiodurans* has evolved to survive severe desiccation, an adaptation that also confers resistance to extraordinary levels of ionizing radiation.[2] Both desiccation and ionizing radiation can leave the cell with hundreds of DNA double-strand breaks,[2] a crisis that the *Deinococcus* RecA protein (DrRecA) appears to handle efficiently.

RecA protein has proven to be indispensable for complete chromosome repair in *D. radiodurans*.[13,15,32,33] RecA plays a role in both of the two central processes of genome reconstitution in *D. radiodurans*.[13−15] The ESDSA phase may be initiated in part by DrRecA binding to the end of double-strand DNA to partially unwind the DNA and provide a substrate for an exonuclease like RecJ.[13,15] In the second phase, RecA-dependent homologous recombination is promoted to link many large DNA fragments produced by ESDSA into an intact circular chromosome.[13,14] The pathway of strand exchange in *D. radiodurans* is also started by formation of RecA filaments on dsDNA and then targeting of homologous ssDNA.[34] As a result, unlike that of *E. coli*,[19,20] the functional RecA filament of *D. radiodurans* is most often formed on dsDNA. Therefore, how DrRecA forms nucleoprotein filaments on dsDNA is of substantial interest.

Here, we used a single-molecule approach to examine RecA filament formation. We immobilized one end of dsDNA on a surface and attached the other end to a bead. The approach takes advantage of the properties of RecA, in which binding to dsDNA leads to a 1.5-fold increase in length and an increase in filament stiffness.[35,36] This in turn leads to a measurable change in the bead's Brownian motion (BM). The method of tethered particle motion (TPM) has been widely used in single-molecule studies, addressing problems such as the size of a loop formed by a repressor,[37,38] the folding and unfolding state of G-quadruplex,[39] and translocation on DNA by polymerases[40] and RecBCD helicase/nuclease.[41] By dissecting how the RecA−dsDNA filament is formed, we hope to shed light on RecA adaptations to different repair contexts.

MATERIALS AND METHODS

Single-Molecule Experiments. Duplex DNA with lengths of 99, 186, 382, 427, and 537 bp were prepared by polymerase chain reaction (PCR) with a 5′-digoxigenin-labeled primer and a 5′-biotin-labeled primer using pBR322 templates. PCR products were gel purified. Slides and streptavidin-labeled beads (200 nm, Bangs laboratories) were prepared as described previously.[39,42] Individual dsDNA molecules were tethered on the antidigoxigenin-labeled slide, and the other ends of the DNA molecules were attached to streptavidin-labeled beads for visualization. The level of nonspecific interaction between the beads and the slide surface is reduced by using BSA (Calbiochem) as a carrier protein included in all buffers.

For the Brownian motion (BM) dependence of various duplex DNA lengths (Figure 1b), DNA of specific lengths (1 nM molecules), RecA (2 μM), and ATPγS [2 mM, containing <10% ADP (Roche)] were incubated for more than 2 h at room temperature to ensure the DNA molecules were fully coated by RecA molecules. More than 100 tethers were collected (for dsDNA and the RecA−dsDNA complex) with each tether's BM values derived by analyzing the standard deviation of 500 constructive frames (30 Hz). The error bars indicate the standard deviation.

For real-time RecA nucleation and extension observations, the 382 and 186 bp duplex DNA molecules were used for EcRecA and DrRecA, respectively, unless indicated otherwise. EcRecA was purchased from New England Biolabs without further purification, and DrRecA was purified as previously described.[43] 1000 frames (~33 s) were recorded to establish the BM of the unbound dsDNA before flow in a 40 μL mixture of RecA (2 μM) with specific nucleotides [ATP or ATPγS, 2 mM (Sigma)]. When ATP was used, an ATP regenerating system [10 units/mL pyruvate kinase and 3 mM phosphoenolpyruvate (Sigma)] was included. All reactions were conducted at 22 °C. Two additional experiments were conducted using the buffer condition that was used in a previous study[44] [buffer A (pH 6.20): 1 mM $Mg(OAc)_2$, 20 mM MES, 20% sucrose, 30 mM dithiothreitol, and 0.5 mM ATP, but with 1 mg/mL BSA added to avoid nonspecific interaction]. Except for the experiment with DrRecA at pH 6.46, which included a different buffer (buffer C: 20 mM ACES, 5% glycerol, 10 mM $Mg(OAc)_2$, 3 mM potassium glutamate, 1 mM DTT, and 1 mg/mL BSA), all reactions were conducted in buffer B, containing 25 mM MES, 5% glycerol, 10 mM $Mg(OAc)_2$, 3 mM potassium glutamate, 1 mM DTT, and 1 mg/mL BSA at the indicated pH.

For the experiment showing the time-dependent change of the BM distribution of EcRecA and DrRecA (from 0 to 30 h), DrRecA and EcRecA were both studied using 382 bp dsDNA at pH 6.06, in buffer B but with 4 mM ATP and 0.2 mM ATPγS mixed. More than 100 tethers were collected at each time (0, 1, 5, 10, and 30 h), with each tether's BM values derived by analyzing the standard deviation of 500 constructive frames (30 Hz).

Statistical Analysis. The microscope setup and imaging acquisition were previously described.[39,42] The image was captured at a rate of 33 ms/frame. The effect of thermal drift was excluded by measuring tethering bead positions relative to beads prefixed on the slide. To ensure that there is only one DNA molecule attached to each bead, only the beads with symmetrical BM (x/y ratio between 0.9 and 1.1) were analyzed. Therefore, the standard deviation based on y is the same as that based on x. For time course measurements, 40 consecutive frames (1.3 s) were used to calculate the x standard deviation of the bead distribution, which in turn reflects the amplitude of BM of the DNA tethers. Using more frame numbers does not alter the value. These time courses were then used to determine the nucleation time, extension rates, and maximum BM of RecA assembly along duplex DNA.

For nucleation, the intrinsic uncertainty of naked dsDNA's BM constrained our resolution. The BM distribution of naked dsDNA for 33 s showed that we cannot distinguish BM changes associated with fewer than 12 or 6 RecA subunits bound for the 382 or 186 bp dsDNA, respectively.

The averaged nucleation times were derived from exponential fitting using Origin 8. Panels a−c of Figure 2 show the best fitting derived from the formula $y = y_0 + A \times \exp(-t/\tau)$, and all exhibited a very small y_0 (<1% maximum value of y). The fitted nucleation times were similar to those fitted by the formula $y = A \times \exp(-t/\tau)$ and the maximum likelihood estimation (see Figure S1b of the Supporting Information for more detail).

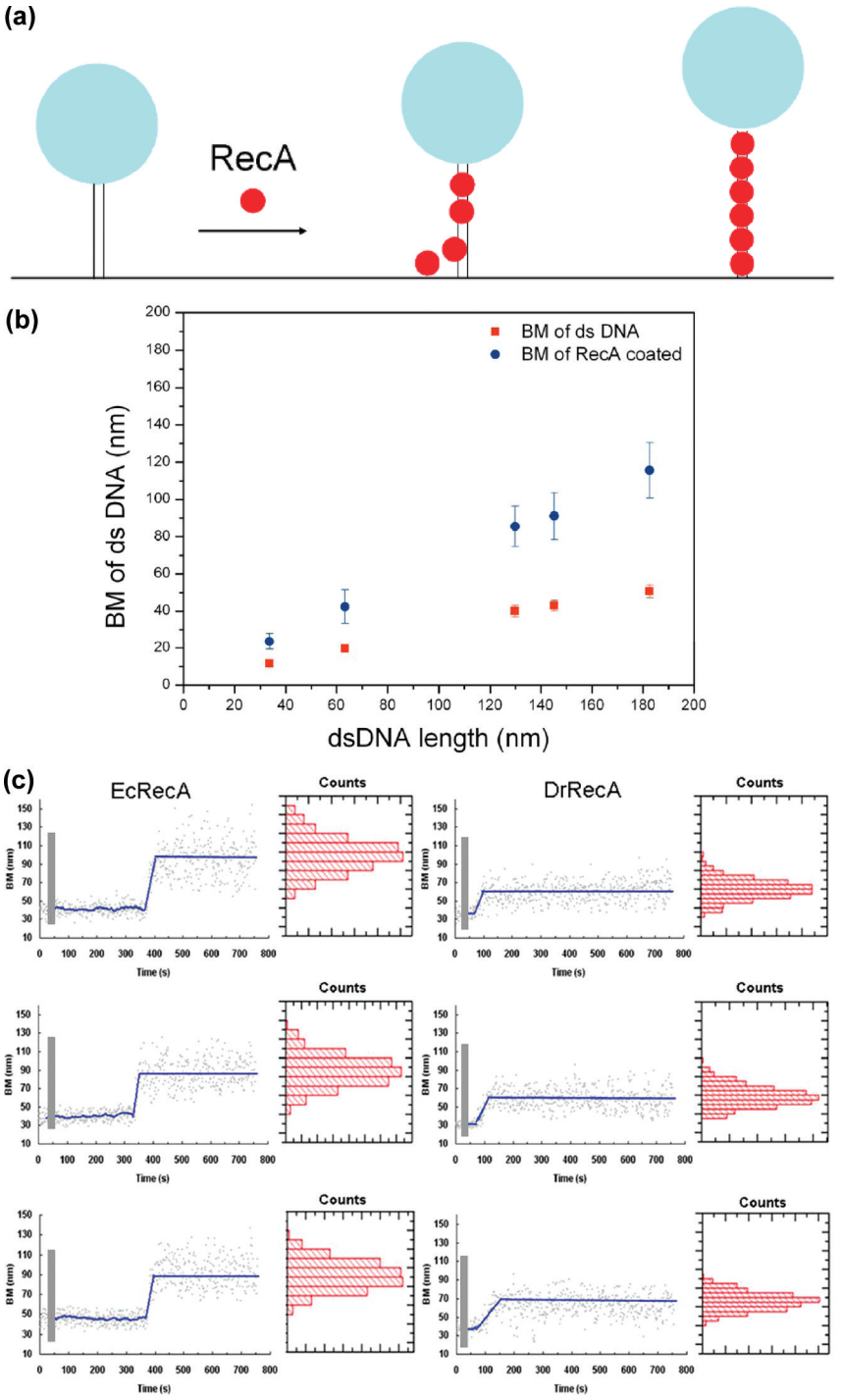

Figure 1. Observation of RecA assembly along a single duplex DNA molecule using TPM experiments. (a) Changes in bead Brownian motion amplitude reflect the real-time dynamics of RecA nucleation and extension processes. (b) The amplitude of a bead's BM is found to be proportional to bare DNA length (■) within the DNA size studied. The stable extended EcRecA–dsDNA filaments in the presence of the nonhydrolyzable ATP analogue, ATPγS (●), show a similar linear DNA length dependence, but with a larger slope. Each point contains data from more than 200 tethers, and error bars indicate the standard deviation. (c) Representative time traces of RecA assembly on a single 382 bp duplex DNA molecule in buffer B at pH 6.16 and 2 mM ATP. The left column is for samples that contained traces of EcRecA and the right column for samples that contained DrRecA. The gray bar designates the time of RecA addition and system restabilization (~9–11 s). The recordings were continuous during the buffer change, so the same DNA tethers were monitored throughout the reaction. The time between RecA flow in and Brownian motion change is regarded as the nucleation time (the blue line was fit with a moving average adjoining 20 points). The phase in which the bead BM showed a continuous increase is defined as extension and is fitted with the method described in Statistical Analysis. We defined the final BM plateau as the maximum BM achieved. BM values of the plateau were collected, and the histograms are shown beside each time trace. The blue line of the final part indicates the BM of the Gaussian peak.

We defined the time from the moment we added RecA to the moment the BM began to continuously increase, distinguished from the intrinsic uncertainty of the BM derived from naked dsDNA, as the nucleation time. The nucleation times of many

dx.doi.org/10.1021/bi200423t | *Biochemistry* 2011, 50, 8270–8280

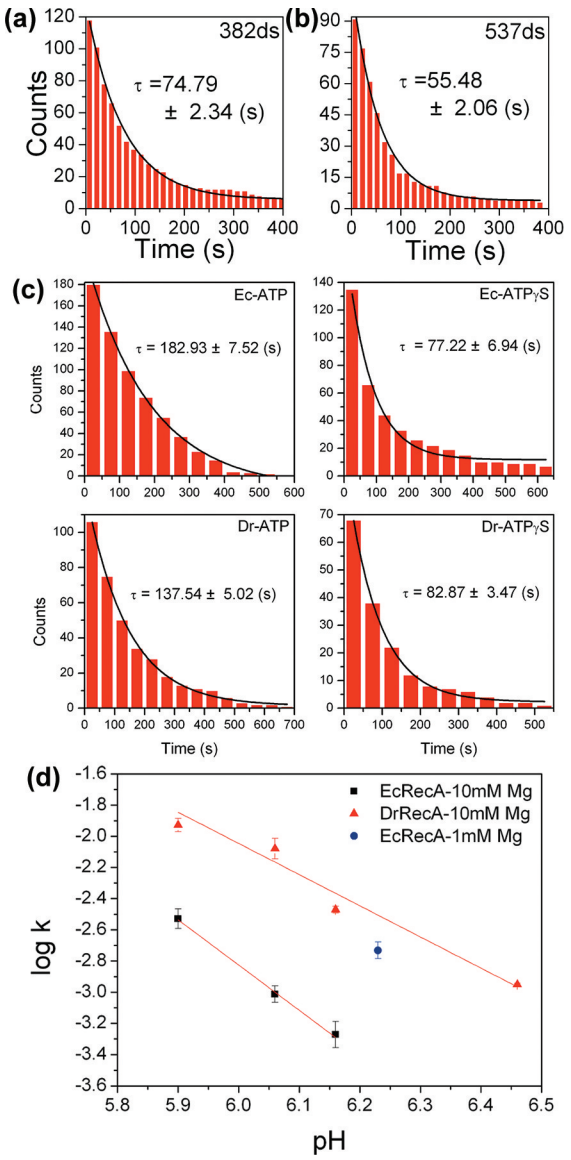

Figure 2. Measured nucleation times using TPM. Nucleation times from individual time courses were binned into a cumulative plot and fitted by a single exponential. (a) EcRecA nucleation with 382 bp dsDNA under the same buffer condition described by Galletto et al.[44] (buffer A). The fitted time is 74.79 ± 2.34 s (N = 118). (b) EcRecA nucleation with 537 bp dsDNA under the same buffer condition described by Galletto et al. (buffer A). The fitted time is 55.48 ± 2.06 s (N = 91). (c) Nucleation time for EcRecA and DrRecA with 382 bp dsDNA in the presence of different nucleotides, ATP and ATPγS. EcRecA was under buffer B (pH 6.06) and 2 mM ATP (or ATPγS). The nucleation time is 182.93 ± 7.52 s (N = 180) with ATP and 77.22 ± 6.94 s (N = 135) with ATPγS. DrRecA was used in buffer C (pH 6.46) and 2 mM ATP (or ATPγS). The nucleation time is 137.54 ± 5.02 s (N = 106) with ATP and 82.87 ± 3.47 s (N = 68) with ATPγS. (d) Nucleation rates (in units of bp^{-1} min^{-1}) of EcRecA (squares) and DrRecA (triangles) in buffer B using ATP at different pH values. The slopes of these two lines are −2.90 and −2.0 for EcRecA and DrRecA, respectively. The nucleation rate of EcRecA shown in panel a is also shown in panel d to provide a direct comparison (circles). The data reported were from the analysis of nucleation times of more than 100 tethers, and the error bars reflect the deviation using either a single-exponential fitting or the maximum likelihood estimation (see Figure S1b of the Supporting Information for more detail).

tethers were collected in a cumulative histogram and then fitted with a single exponential to derive the average nucleation time. Varying the bin size of the cumulative plot changes the value only within the fitting error. Earlier studies established that EcRecA forms a stable nucleus on DNA when ~6 RecA subunits are assembled,[22,44] so our nucleation time also includes a minimal degree of extension as well because of the resolution discussed above. However, if the extension time of 6−12 RecA subunits is taken into account using the previously reported EcRecA extension rates[22,44,49,50] (or using our determined rates in this work), it also only changes the nucleation time value within the fitting error.

Considering how much time it takes for RecA to fully coat the nucleoprotein filament, we can directly compare the extension rate of EcRecA with that of DrRecA. Figure S2 of the Supporting Information shows extension rate distributions calculated by dividing the number of RecA subunits (one-third of nucleotides) by the extension duration time. We also used a linear fitting to the continuously increasing BM time course (the slope) to calculate the extension rates (Figure S2 of the Supporting Information). Both analyses returned a similar distribution within our resolution. We thus report the fitted slopes of the continuous BM rise segments in the reaction traces as extension rates. Conversion factors relating BM to the number of bound RecA subunits for various DNA lengths were obtained by dividing the number of bound RecA subunits at saturation (equal to one-third of the number of base pairs in the duplex DNA molecule) into the BM difference observed between the BM of naked dsDNA and the final (maximum) BM observed in Figure 1b (Figure S3 of the Supporting Information). Because the size of DrRecA is similar to that of EcRecA and both of them formed similar filaments at the end (see further discussion in Figure 5), this factor was used for both EcRecA and DrRecA.

Defined slopes could vary, depending on the exact starting and end point of the fitting region, but all rates showed variation no larger than 0.31 RecA/s (after unit conversion), which is within the bin size (0.5 RecA/s) of the rate distribution.

For the maximum BM achieved, the plateau BM values of every single trace were fitted with a Gaussian, and we regarded the peak as the maximum BM achieved for each tether.

Electron Microscopy. A modified Alcian method was used to visualize RecA filaments. Activated grids were prepared as previously described.[45] EcRecA or DrRecA protein (0.8 μM) was preincubated with 12 μM (in nucleotides) Nb.BsmI nicked circular double-stranded M13mp18 DNA in buffer B (pH 6.06) for 10 min at room temperature. An ATP regeneration system of 10 units/mL creatine phosphokinase and 12 mM phosphocreatine was also included in the incubation. ATP was added to a final concentration of 0.8 mM, and the reaction mixture was incubated for an additional 15 min. ATPγS was then added to a final concentration of 0.8 mM to stabilize the filaments, followed by incubation for 5 min.

The reaction mixture described above was diluted 2-fold with 200 mM ammonium acetate, 10 mM MES (pH 6.06), and 10% (v/v) glycerol and adsorbed to an activated carbon grid (Alcian grid) for 3 min. The grid was then touched to a drop of the buffer described above, followed by floating on a second drop of the buffer for 1 min. The sample was then stained by being touched to a drop of 5% uranyl acetate followed by floating on a fresh drop of a 5% uranyl acetate solution for 30 s. Finally, the grid was washed by being touched to a drop of doubly distilled water followed by successive immersion in two 10 mL beakers of doubly distilled water. After the sample was dried, it was

dx.doi.org/10.1021/bi200423t | Biochemistry 2011, 50, 8270–8280

rotary-shadowed with platinum. This protocol is designed for visualization of complete reaction mixtures, and no attempt was made to remove unreacted material. Although this approach should yield results that provide insight into reaction components, it does lead to samples with a high background of unreacted proteins.

Imaging and photography were conducted with a TECNAI G2 12 Twin Electron Microscope (FEI Co.) equipped with a GATAN 890 CCD camera. Digital images of the nucleoprotein filaments were taken at 15000× magnification. Filament fragment lengths (protein-coated regions of DNA) were measured using MetaMorph analysis software. Circular DNA molecules that contained protein were measured and analyzed, a total of 28 from EcRecA and 27 from DrRecA samples. Each filament fragment was measured three times, and the average length was calculated. The 500 nm scale bar was used as a standard to calculate the number of pixels per nanometer. Each nucleoprotein fragment length, originally measured by MetaMorph in pixels, was thus converted to nanometers.

RESULTS

RecA Assembly Dynamics Studied by TPM Experiments. When RecA recombinases form nucleoprotein filaments on duplex DNA, the DNA within the filaments is underwound and the end-to-end distance of DNA increases approximately 50%.[36,46] In addition to increasing the DNA length, binding of RecA also stiffens DNA, resulting in a more rigid DNA−RecA complex.[23] The persistence length is increased from a value of ∼50 nm typical of duplex DNA to a value of 464 nm measured for RecA nucleoprotein filaments.[47] We have devised a TPM approach for the examination of RecA filament formation at the single-molecule level.

In the TPM measurement, individual duplex DNA molecules were immobilized on the glass surface through a digoxigenin−antidigoxigenin linkage. The distal end of the DNA was linked to a streptavidin-labeled bead that could be viewed by differential interference contrast (DIC) light microscopy (Figure 1a). In solution, the segment of DNA between the bead and the surface attachment acts as a flexible tether that constrains the bead BM to a small region above the glass surface. Changes in the length and rigidity of the DNA tether result in a change in the spatial extent of bead BM. This change in bead motion can be measured to nanometer precision using digital image processing techniques that determine the standard deviation of the bead centroid position in light microscope recordings.[39,41,42,48] Figure 1b shows that the bead BM before and after EcRecA coating is distinguishable for a series of dsDNA lengths.

Typical time courses of EcRecA assembly on a 382 bp duplex DNA are shown in the left column of Figure 1c. After a 1000-frame (33 s) recording of the BM of dsDNA tethers, a mixture of EcRecA and ATP (or ATPγS) was introduced into the reaction chamber, as shown by the gray bar, with a dead time of ∼10 s due to focus restabilization. The same DNA tether was recorded to monitor the RecA assembly process. In Figure 1c, the DNA tether length remained constant until reaching a point where an obvious, continuous increase in BM was observed. The DNA tether length then remained constant at the higher BM amplitude, consistent with the BM value we measured for fully coated EcRecA−dsDNA filaments in Figure 1b.

We define the dwell time between the introduction of RecA and the time at which apparent BM change occurred as the nucleation time, the continuous BM increase region as the DNA extension caused by RecA assembly, and the high BM value at which DNA tether length remained constant as the maximum BM achieved. For the study described below, experiments and analysis were first conducted with EcRecA, and results were compared with those of previous reports to validate the TPM experiments. We then applied this method to study DrRecA filament formation. Finally, we confirmed these results with electron microscopy studies.

DrRecA Nucleates Faster Than EcRecA on dsDNA. The time from the moment RecA was added to the reaction mixture (flowed in) to the moment a continuous increase in BM was observed that could be distinguished from the intrinsic uncertainty of naked dsDNA was defined as the nucleation time. The nucleation times of many tethers were collected in a cumulative histogram and then fitted with a single exponential to derive the average nucleation time (Figure 2).

We first conducted a series of experiments to verify that TPM methods are capable of monitoring the nucleation time of RecA. First, longer dsDNA molecules provide more sites for nucleation and would thus reduce the nucleation time. EcRecA assembly was studied using 382 bp (Figure 2a) and 537 bp (Figure 2b) dsDNA under the same buffer condition. A shorter nucleation time was indeed observed for longer DNA but with a similar nucleation rate (number of nucleation events per base pair of DNA per minute). Second, previous reports documented that EcRecA nucleates faster in the presence of ATPγS than in the presence of ATP.[44,50,51] The faster nucleation is thought to result from the higher affinity of RecA protein for ATPγS.[44] Using the 382 bp dsDNA, we determined that the nucleation time is indeed shorter in the presence of ATPγS than in the presence of ATP (Figure 2c). Third, we also examined the pH dependence on the nucleation rate of EcRecA proteins [Figure 2d (squares)]. EcRecA nucleation on fully dsDNA became slower at higher pH values (>6.5),[21,51] with a slope of −3.03. This is consistent with the studies conducted by Pugh and Cox,[21] which showed that EcRecA takes up three protons during nucleation.[21] Finally, the nucleation rate at 1 mM Mg^{2+} [Figure 2d (circles)] was faster than that at 10 mM Mg^{2+} (squares). This result is again consistent with the notion that the level of binding of RecA to dsDNA is inversely proportional to DNA stability.[53] Applying force by stretching DNA,[54] increasing temperature,[53] or decreasing cation concentration[53] weakens the thermal stability of dsDNA and thus facilitates RecA binding and augments the RecA nucleation rate.

EcRecA nucleation rates determined using the 382 bp dsDNA (Figure 2a) were studied using buffer conditions similar to those used in an earlier report using much longer DNAs,[44] but the nucleation rate was somewhat higher than those previously reported.[44,50] With the knowledge that TPM experiments accurately describe RecA assembly behaviors as listed above, the current reported nucleation rates actually reflect the improved sensitivity and resolution of the TPM experimental design. The spatial resolution of earlier studies is in the range of hundreds of nanometers, because of the long DNA molecules used (lambda DNA, 48 kb) and the diffraction limit posted by fluorescence imaging.[44,50] Moreover, as observed by Hilario et al., small amounts of detached RecA during repetitive translation of the DNA filament between the reaction channel and the observation channel may also exert a small delay on nucleation.[55] Using much shorter DNAs (hundreds of base pairs), TPM experiments offer improved sensitivity and higher resolution, so the RecA nucleation time can be determined more accurately.

We next examined the nucleation process of DrRecA on dsDNA. Experiments with DrRecA using the 382 bp dsDNA indicated that nucleation was too fast to accurately determine the nucleation time at lower pH values, mainly because of the 10 s dead time for instrument restabilization after the introduction of RecA. Because the nucleation time depends on the number of available nucleation sites (the DNA length) and pH, the work with DrRecA thus required a higher pH or a shorter DNA to slow the nucleation process. Experiments were first conducted at pH 6.46. We then extended these measurements to lower pH values by using shorter DNA molecules. As with EcRecA,[44,50,51] DrRecA also nucleates faster in the presence of ATPγS than in the presence of ATP (Figure 2c). The inverse DNA length dependence of nucleation times also holds for DrRecA (Figure S1a of the Supporting Information). DrRecA nucleation rates were determined with a shorter DNA of a 186 bp duplex at the same pH values used for the EcRecA. All nucleation rates are reported in terms of the number of nucleation events per base pair per minute for direct comparison between EcRecA and DrRecA (Table 1). DrRecA

Table 1. Direct Comparison between DrRecA and EcRecA at a Series of Different pH Values

	nucleation rate under ATP (bp^{-1} min^{-1})			
	pH 5.90	pH 6.06	pH 6.16	pH 6.46
DrRecA	1.30×10^{-2}	9.24×10^{-3}	3.51×10^{-3}	1.14×10^{-3}
EcRecA	2.68×10^{-3}	8.59×10^{-4}	4.41×10^{-4}	

exhibited a much faster nucleation rate than EcRecA at the various pH values we examined. Moreover, the pH dependence studies of DrRecA imply that DrRecA takes up approximately two protons during nucleation [Figure 2d (triangles), slope of −1.93]. The difference of one proton taken up during nucleation between EcRecA and DrRecA (three for EcRecA and two for DrRecA) increases the difference between nucleation rates even more at higher pH values. Because the DNA we used is short (hundreds of base pairs), it was not feasible to measure the slow nucleation rates at higher pH values on the experimental time scale. Thus, real-time TPM detection is only conducted at lower pH values. Strand exchange is promoted over the pH range of 6.0−8.4,[52] and results here permit an estimation of nucleation rates at higher pH values (the condition at which strand exchange happens with optimal efficiency) by extrapolation of the measurements in Figure 2d.

DrRecA Extends Its Filaments More Slowly Than EcRecA. The continuous BM increase in Figure 1c represents the extension process of RecA assembly. We calculated the extension rates on the basis of two different methods: the dwell time required for full filament assembly and the linear fitting of the continuously increasing BM time course (the slope), as shown in Figure S2 of the Supporting Information. Both analyses returned with a similar extension rate distribution within our experimental resolution. In addition, the extension rates determined here for EcRecA are consistent with what has been previously reported.[44] We thus used the slope of the linear phase corresponding to the continuous BM increase to define extension rates for the purposes of this study. Even though we cannot completely exclude potential error associated with slope fitting, particularly the possibility that the relation between RecA binding and the observed BM is not perfectly linear, the slopes of all BM increases were linear within the experimental

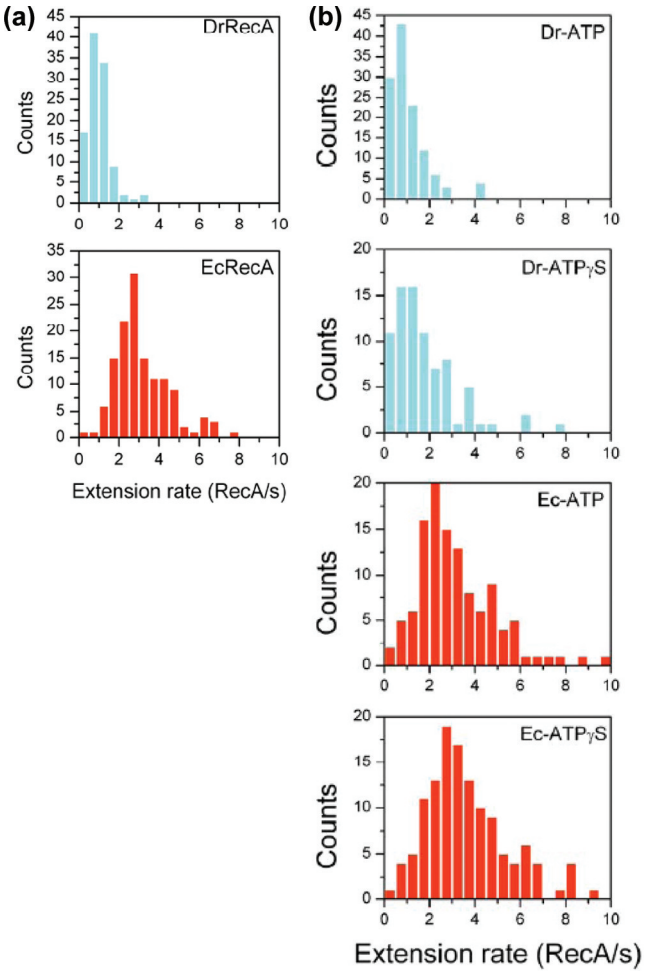

Figure 3. Observed extension rates. (a) Rate distribution of DrRecA and EcRecA with 382 bp dsDNA in buffer B (pH 6.16) and 2 mM ATP (N = 106 for DrRecA; N = 135 for EcRecA). (b) Rate distribution of DrRecA and EcRecA with ATP and ATPγS using 382 bp dsDNA. EcRecA was studied in buffer B (pH 6.06) with 2 mM ATP (or ATPγS), and DrRecA was studied in buffer C (pH 6.46) with 2 mM ATP (or ATPγS).

limits of these observations, and any nonlinearity is thus small and constrained by those limits.

Slopes defined could vary, depending on the exact starting and end point of the fitting region, but all rates showed variation no larger than 0.31 RecA/s (after unit conversion), which is within the bin size (0.5 RecA/s) of the rate distribution. There are a few factors that might lead to an overestimation. We cannot entirely exclude the possibility of multiple nucleation events occurring during the extension process. However, the typical nucleation times (e.g., see Figure 1c) were sufficiently long for EcRecA that multiple nucleations are considered unlikely, except in cases where one nucleation event in the middle of the DNA stimulates a second event at the same site. The slow nucleation of EcRecA onto dsDNA was previously shown to be tightly linked to DNA underwinding,[21,51] such that any structural perturbation or feature that rendered the DNA easier to unwind also facilitated nucleation. For example, nucleation events on a linear duplex DNA are thus most likely to occur at DNA ends where the strands are more readily separated and at regions of high A/T content in the sequence. In our experiments, DNA ends are attached to a bead or the slide; thus, the potential for

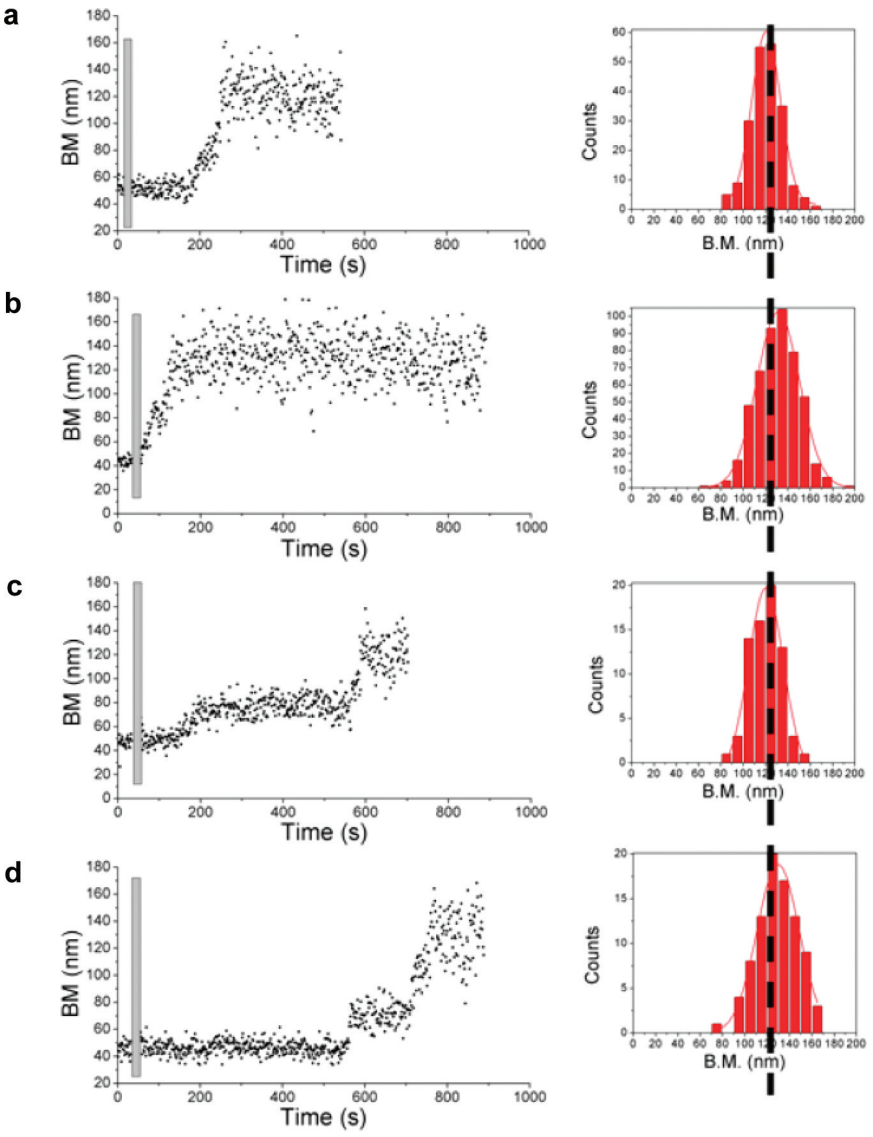

Figure 4. Final BM achieved is a characteristic factor. Four traces of EcRecA with 537 bp dsDNA in buffer B (pH 6.16) with 2 mM ATPγS are shown. Histograms show the final BM values achieved for each experiment. The results in panels a–d show that no matter how the RecA filament forms, the final BM achieved did not vary (histograms).

perturbation is somewhat different. Once a filament segment has been nucleated at a position in the DNA interior, the DNA within the filament is underwound, and winding of the DNA immediately adjacent to the filament should be affected. Thus, the nucleating end of one filament may represent an enhanced nucleation site for another nucleation event, adjacent to the first filament and sometimes oriented in the opposite direction. This second event would thus complete the binding of the DNA. Two nearly simultaneous nucleation events would give rise to a doubling of the observed slope of BM increase and lead to an overestimation of the normal rate by a factor of 2. On the other hand, if there were pauses between two separate extension phases on one DNA molecule that could not be distinguished within our experimental resolution, these pauses could lead to a small underestimation of the rate.

Although the limitations described above existed, rates of extension of EcRecA derived from our experiments were all within the range of rates that have been reported.[44,49,50] Varying the buffer conditions does not significantly alter the extension rates (Figure S4 of the Supporting Information), as we expected that extension is relatively independent of the salt condition and pH value on the basis of previously published results.

Extension rates were next examined for DrRecA. The extension rate distribution also shows negligible variation at different pH values (Figure S5 of the Supporting Information), consistent with what is shown for EcRecA. To exclude any influence of DNA length and pH, we directly compared extension rates between EcRecA and DrRecA at the same pH (pH 6.16, with ATP) with the same length of dsDNA (382 bp). Figure 3a shows that DrRecA extends more slowly than EcRecA. Experiments were also conducted with ATPγS to test if the extension process was affected by ATP hydrolysis. Because DrRecA nucleates faster with ATPγS (Figure 2c), an accurate measurement must be taken at higher pH values. However, EcRecA nucleates too slowly for real-time observation under the same high-pH condition for direct comparison. Therefore, considering that the extension rate distribution is independent of pH, we measured the rate distributions for filament extension with ATP or ATPγS at pH 6.06 for EcRecA

dx.doi.org/10.1021/bi200423t | *Biochemistry* 2011, 50, 8270–8280

and pH 6.46 for DrRecA. In Figure 3b, we show that the extension rate distributions changed very little for ATP and ATPγS, and EcRecA has faster extension rates than DrRecA in both nucleotide states. This confirms that DrRecA exhibits a slower extension rate than EcRecA and this rate is independent of ATP hydrolysis.

DrRecA Forms a Filament with One or More Gaps. RecA nucleoprotein filament formation starts when RecA nucleates on any site along dsDNA, followed by extension. If RecA nucleates in the middle of dsDNA but another nucleation event does not happen until the first filament extends unidirectionally along one strand to one end or the other, then a two-step extension might be observed. A small number of apparent two-step extension events were observed in our experiments, with the frequency of such events increasing for longer dsDNA molecules. Even with the longest DNA used in our experiment, the fraction of two-step events was small (~10%). A few exemplary time traces with EcRecA and ATPγS assembled on a 537 bp dsDNA are presented in Figure 4. Even though the filaments can form in more than one way, the maximum BM values achieved in Figure 4 are similar for different tethers under the same experimental conditions.

Therefore, the maximum BM achieved can thus be regarded as a characteristic of RecA nucleoprotein filaments. However, because of the different lengths of dsDNA used in this work, we cannot directly compare the maximum BM values for different DNAs. Instead, the ratio of the final and initial BM offers a direct comparison of various filaments, such as EcRecA and DrRecA. Figure 5a shows the extension ratio of EcRecA (filled squares) and DrRecA (filled circles) at different pH values under ATP condition. Even though the extension ratio changes slightly at different pH values, DrRecA always exhibited an extension ratio slightly lower than that of EcRecA. To determine if this resulted from the higher rates of ATP hydrolysis of DrRecA, experiments in the presence of ATPγS were conducted (Figure 5a, empty circles and squares for ATPγS). Figure 5a shows that even with ATPγS, EcRecA still has a higher extension ratio than DrRecA, suggesting that this effect is not mainly caused by ATP hydrolysis. The slightly larger extension ratio seen with ATPγS than that with ATP might be due to a less extended RecA−dsDNA filament in the presence of ATP, consistent with previous studies.[56]

The smaller maximum BM observed for DrRecA may have two possible causes. First, DrRecA may form a somewhat more compact filament than EcRecA, which also results in a smaller observed BM. Second, a filament with one or more gaps that break up its continuity could also lead to a smaller BM. Considering the faster nucleation but slower extension rates of DrRecA, a filament with multiple nucleation events to form short RecA patches along DNA is possible. Because one RecA occupies three nucleotides,[36] there must be a gap between two RecA patches, and the gap size depends on the size of the extension oligomer. If DrRecA is extended by the addition of monomeric subunits, then the maximum gap size is 2 bp, which is too small for us to detect. Therefore, if the smaller BM observed for DrRecA was caused by many gaps within the RecA filament, then it also suggested that DrRecA was extended by addition of multimeric DrRecA units. Electron microscopy images of DrRecA published to date have not produced evidence of a filament more compact than EcRecA.[43] A fast nucleation followed by slow extension, especially extension by means of the addition of multimers, does produce a less continuous filament for Rad51.[57] All of these

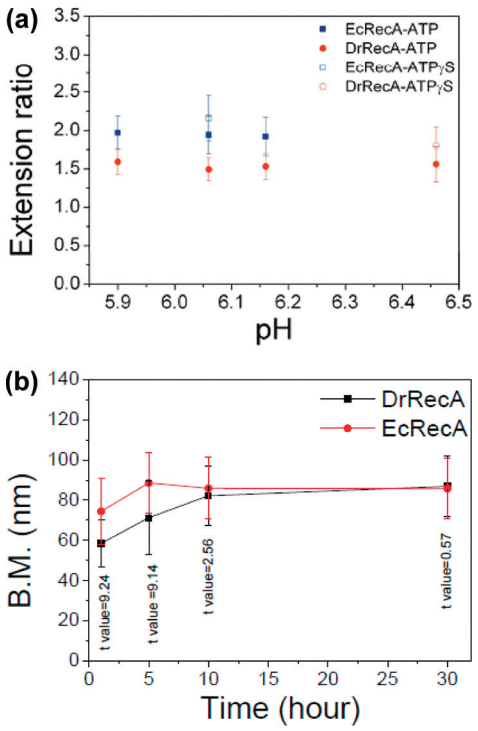

Figure 5. Maximum amplitude of bead BM upon RecA assembly. (a) The extension ratio provides a direct comparison between different DNA length observations of EcRecA and DrRecA: (filled squares) EcRecA with ATP, (filled circles) DrRecA with ATP, (empty squares) EcRecA with ATPγS, and (empty circles) DrRecA with ATPγS. Error bars indicate the standard deviation. (b) Extended time observation of BM of EcRecA and DrRecA filaments. Experiments with DrRecA and EcRecA were both conducted with the 382 bp dsDNA with buffer B (pH 6.06) with 4 mM ATP and 0.2 mM ATPγS. More than 100 tethers were collected at each time (0, 1, 5, 10, and 30 h) to analyze their BM. *t* values are labeled.

observations suggest that the somewhat lower BM reflects the formation of DrRecA filaments with one or more gaps of significant size.

If the lower BM simply reflects a more compact filament, then the length of the filament and the observed BM should not change with time. However, if filaments typically include one or more gaps, a slow redistribution of RecA subunits with time could generate a more continuous filament with a correspondingly slow increase in BM. We followed the BM values of both EcRecA and DrRecA filaments using 382 bp DNA substrates at various time points that are sufficiently long for RecA dissociation and binding to occur. The reaction was conducted in a mixture of ATP and ATPγS, with the ATP concentration being 20 times higher than the ATPγS concentration. The high concentration of ATP allowed us to provide enough time for RecA binding and limited dissociation. The accompanying low concentration of ATPγS prevented RecA disassembly after periods of observation. Figure 5b shows the BM distribution of EcRecA and DrRecA assembled on the 382 bp dsDNA at different times. The BM for the DrRecA filaments increased slowly and exhibited essentially the same distribution as that of EcRecA after 30 h. A *t* test was conducted to confirm that the BM distributions of EcRecA and DrRecA were different at first but the same at the end of the observation. This slow increase in BM suggests that DrRecA

dx.doi.org/10.1021/bi200423t | *Biochemistry* 2011, 50, 8270–8280

filaments might contain gaps initially, and DrRecA redistribution allows gap removal and the formation of continuous filaments at later times.

We also used electron microscopy to examine nucleation and extension by DrRecA or EcRecA on dsDNA under very similar reaction conditions. The faster nucleation and slower extension of DrRecA protein filaments should result in larger numbers of shorter filaments; the filaments formed by EcRecA should be longer because of its slow nucleation and fast extension. This would be especially evident under conditions in which RecA protein was present in subsaturating amounts relative to available DNA binding sites. We also expected a larger number of discontinuities (gaps) in the DrRecA protein samples than the EcRecA samples. The protein concentration used in these experiments was sufficient to bind approximately 40% of the available DNA binding sites in the relaxed circular dsDNA. Representative DrRecA and EcRecA nucleoprotein filaments, observed by EM, are shown in panels a and c of Figure 6, respectively. Among the 27 DrRecA–dsDNA molecules analyzed, we counted a total of 368 nucleoprotein fragments and on average 14 gaps per DNA molecule. The DrRecA fragments were mostly short (mean of 151.6 nm), with only one filament segment measuring more than 1000 nm (Figure 6b). Among the 28 EcRecA–dsDNA molecules analyzed, approximately four gaps were found in each molecule. This resulted in 113 fragments that were relatively long, varying in size from 31.64 to 2599 nm (Figure 6d). The average EcRecA filament segment length was 745.6 nm, almost 5 times longer than the average DrRecA filament segment.

DISCUSSION

We have examined the process of RecA binding to dsDNA with a single-molecule approach, observing the Brownian motion of a bead connected to one tethered dsDNA. As seen in past studies, the nucleation rate limits the overall rate of RecA filament formation.[53,58] Our work with the EcRecA protein demonstrates that the TPM method produces the same dependences of nucleation and extension rates on pH as previously documented. The absolute rates of nucleation we observed are somewhat faster than those previously reported, likely because of the greater resolution of our method. Most importantly, we demonstrate that the DrRecA protein exhibits important differences from EcRecA in binding to dsDNA, nucleating faster, extending slower, and resulting in a RecA filament less continuous than the typical RecA protein, *E. coli* RecA. The overall conclusions reached with the new TPM method were supported by the results of electron microscopy experiments conducted in parallel.

The RecA proteins derived from different bacterial species tend to exhibit little obvious variation, forming similar filaments on DNA and conducting a similar set of reactions.[1,16] Adaptations to different cellular DNA repair contexts are likely to be found in the details, particularly the details of filament formation, kinetics, and stability. The parameters we define here for the formation of DrRecA filaments on DNA may reveal some information about how the RecA protein of *D. radiodurans* operates in an environment requiring the repair of many double-strand breaks at one time. Fast nucleation and slow extension make sense in this context, potentially leading to many shorter filaments (rather than a few long ones) and a more productive deployment of the protein for repair.

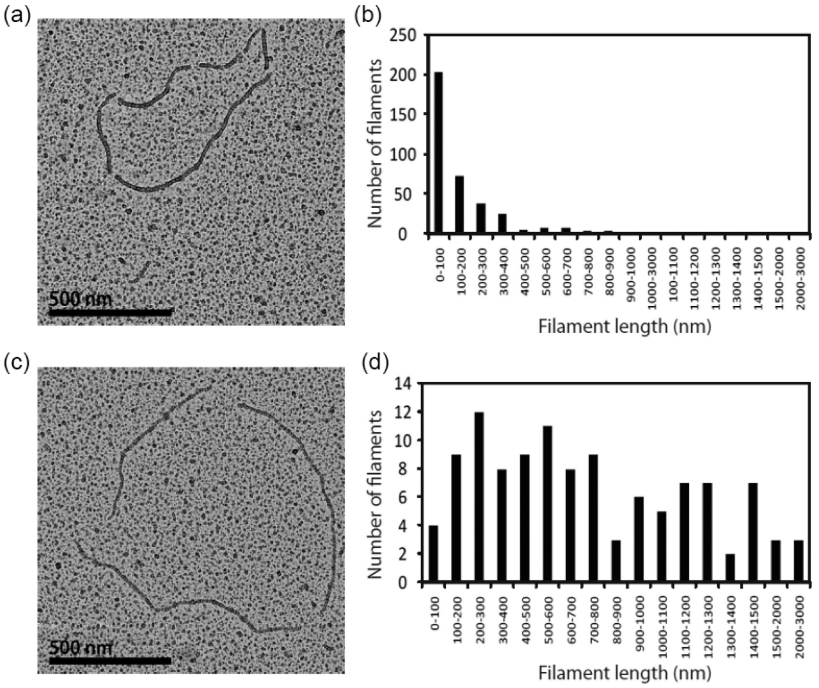

Figure 6. DrRecA formed more gaps and much shorter nucleoprotein filaments than EcRecA as visualized by electron microscopy. Reactions were conducted as described in Materials and Methods. (a) Representative circular dsDNA bound by DrRecA containing six gaps and six nucleoprotein filaments. (b) Quantification of 27 circular dsDNA molecules bound by DrRecA shows that DrRecA forms a total of 368 short filaments within that population, most of which are very short. (c) Representative circular dsDNA bound by EcRecA containing three gaps and three nucleoprotein filaments. (d) Quantification of 28 circular dsDNA molecules bound by EcRecA shows that EcRecA forms 113 nucleoprotein filaments that vary from short to very long, up to 2599 nm.

As with any experimental approach, including single-molecule approaches, our method has some limitations. The nucleation rate may be slightly faster than we report, because we cannot detect fewer than 12 or 6 bound RecA subunits depending on the DNA substrate and conditions. We also cannot entirely exclude the occurrence of multiple nucleation events that would lead to a higher apparent extension rate. However, the error in this case should be a factor of no more than 2. The limitations are the same for any RecA protein that might be examined, so that comparisons still provide useful information, especially when the properties of two different RecA proteins are qualitatively discussed.

The apparently fast nucleation observed for DrRecA must be embedded in its structure. We note that the last few amino acids of the C-terminal domain of EcRecA exhibit a high density of negative charges.[16,18,45] A faster binding for RecA to dsDNA can be facilitated by removing these negatively charged residues or stabilizing these negatively charged residues with protons at low pH values.[59,60] The C-terminal domain of DrRecA possesses fewer negative charges,[61] a structure that might contribute to the more rapid nucleation. Moreover, the nucleation rate changes less as a function of pH. With our short dsDNA, we cannot directly provide the nucleation rate at high pH values. However, by extrapolating the rate from our experiments, we can suggest that even at high pH values (7.5−8.5), nucleation would occur rapidly (in the range from several seconds to a few minutes) for DrRecA nucleating on dsDNA fragments generated by radiation (20−30 kb)[13,14] to form a filament. The results are also consistent with the lack of EcRecA binding seen at high pH,[21,51] which facilitates the strand exchange process by not blocking dsDNA with bound RecA. In contrast, DrRecA can easily bind to dsDNA even at high pH, as noted previously.[34] We speculate that the slower filament extension reaction may reflect the presence of 12 extra residues in the N-terminal domain of DrRecA relative to EcRecA.[61] The N-terminal domain packs against part of the core of the adjacent RecA subunit in a RecA filament,[16] and the N-terminal domain must undergo a change in conformation or orientation in the process of filament assembly that may affect extension rates.

■ ASSOCIATED CONTENT

Supporting Information

Additional experimental observations. This material is available free of charge via the Internet at http://pubs.acs.org.

■ AUTHOR INFORMATION

Corresponding Author

*E-mail: hwli@ntu.edu.tw. Phone: +886-2-33664089. Fax: +886-2-23636359.

Funding

This work was supported by the National Science Council (NSC) of Taiwan (H.-W.L.) and the National Institutes of Health (Grant GM32335 to M.M.C.).

■ ACKNOWLEDGMENTS

We thank Mr. Wayne Mah and Axel Brilot for initial pilot work.

■ ABBREVIATIONS

Ec, *E. coli*; Dr, *D. radiodurans*; BM, Brownian motion; TPM, tethered particle motion; ssDNA, single-stranded DNA; dsDNA, double-stranded DNA.

■ REFERENCES

(1) Cox, M. M., and Battista, J. R. (2005) *Deinococcus radiodurans*. The consummate survivor. *Nat. Rev. Microbiol. 3*, 882−892.

(2) Mattimore, V., and Battista, J. R. (1996) Radioresistance of *Deinococcus radiodurans*: Functions necessary to survive ionizing radiation are also necessary to survive prolonged desiccation. *J. Bacteriol. 178*, 633−637.

(3) Levin-Zaidman, S., Englander, J., Shimoni, E., Sharma, A. K., Minton, K. W., and Minsky, A. (2003) Ringlike structure of the *Deinococcus radiodurans* genome: A key to radioresistance? *Science 299*, 254−256.

(4) Englander, J., Klein, E., Brumfeld, V., Sharma, A. K., Doherty, A. J., and Minsky, A. (2004) DNA toroids: Framework for DNA repair in *Deinococcus radiodurans* and in germinating bacterial spores. *J. Bacteriol. 186*, 5973−5977.

(5) Zimmerman, J. M., and Battista, J. R. (2005) A ring-like nucleoid is not necessary for radioresistance in the Deinococcaceae. *BMC Microbiol. 5*, 17.

(6) Daly, M. J., Gaidamakova, E. K., Matrosova, V. Y., Zhai, M., Venkateswaran, A., Hess, M., Omelchenko, M. V., Kostandarithes, H. M., Makarova, K. S., Wackett, L. P., Fredrickson, J. K., and Ghosal, D. (2004) Accumulation of Mn(II) in *Deinococcus radiodurans* facilitates gamma-radiation resistance. *Science 306*, 1025−1028.

(7) Cox, M. M. (2001) Recombinational DNA repair of damaged replication forks in *Escherichia coli*: Questions. *Annu. Rev. Genet. 35*, 53−82.

(8) Minton, K. W. (1996) Repair of ionizing-radiation damage in the radiation resistant bacterium *Deinococcus radiodurans*. *Mutat. Res. DNA Repair 363*, 1−7.

(9) Slade, D., and Radman, M. (2011) Oxidative Stress Resistance in *Deinococcus radiodurans*. *Microbiol. Mol. Biol. Rev. 75*, 133−191.

(10) Daly, M. J., Gaidamakova, E. K., Matrosova, V. Y., Kiang, J. G., Fukumoto, R., Lee, D. Y., Wehr, N. B., Viteri, G. A., Berlett, B. S., and Levine, R. L. (2010) Small-Molecule Antioxidant Proteome-Shields in *Deinococcus radiodurans*. *PLoS One 5*, e12570.

(11) Battista, J. R., Earl, A. M., and Park, M. J. (1999) Why is *Deinococcus radiodurans* so resistant to ionizing radiation? *Trends Microbiol. 7*, 362−365.

(12) Daly, M. J., and Minton, K. W. (1996) An alternative pathway of recombination of chromosomal fragments precedes recA-dependent recombination in the radioresistant bacterium *Deinococcus radiodurans*. *J. Bacteriol. 178*, 4461−4471.

(13) Slade, D., Lindner, A. B., Paul, G., and Radman, M. (2009) Recombination and Replication in DNA Repair of Heavily Irradiated *Deinococcus radiodurans*. *Cell 136*, 1044−1055.

(14) Zahradka, K., Slade, D., Bailone, A., Sommer, S., Averbeck, D., Patranovic, M., Lindner, A. B., and Radman, M. (2006) Reassembly of shattered chromosomes in *Deinococcus radiodurans*. *Nature 443*, 569−573.

(15) Bentchikou, E., Servant, P., Coste, G., and Sommer, S. (2010) A major role of the RecFOR pathway in DNA double-strand-break repair through ESDSA in *Deinococcus radiodurans*. *PLoS Genet. 6*, 2010.

(16) Lusetti, S. L., and Cox, M. M. (2002) The bacterial REcA protein and the recombinational DNA repair of stalled replication forks. *Annu. Rev. Biochem. 71*, 71−100.

(17) Cox, M. M. (2002) The nonmutagenic repair of broken replication forks via recombination. *Mutat. Res. 510*, 107−120.

(18) Cox, M. M. (2007) Regulation of bacterial RecA protein function. *Crit. Rev. Biochem. Mol. Biol. 42*, 41−63.

(19) Cox, M. M. (2007) Motoring along with the bacterial RecA protein. *Nat. Rev. Mol. Cell Biol. 8*, 127−138.

(20) Cox, M. M. (2003) The bacterial RecA protein as a motor protein. *Annu. Rev. Microbiol. 57*, 551−577.

(21) Pugh, B. F., and Cox, M. M. (1988) General mechanism for RecA protein-binding to duplex DNA. *J. Mol. Biol. 203*, 479−493.

(22) Joo, C., Mckinney, S. A., Nakamura, M., Rasnik, I., Myong, S., and Ha, T. (2006) Real-time observation of RecA filament dynamics with single monomer resolution. *Cell 126*, 515−527.

(23) Hegner, M., Smith, S. B., and Bustamante, C. (1999) Polymerization and mechanical properties of single RecA-DNA filaments. *Proc. Natl. Acad. Sci. U.S.A. 96*, 10109−10114.
(24) Cox, M. M. (2000) Recombinational DNA repair in bacteria and the RecA protein. *Prog. Nucleic Acid Res. Mol. Biol. 63*, 311−366.
(25) Michel, B. (2000) Replication fork arrest and DNA recombination. *Trends Biochem. Sci. 25*, 173−178.
(26) Michel, B., Grompone, G., Flores, M. J., and Bidnenko, V. (2004) Multiple pathways process stalled replication forks. *Proc. Natl. Acad. Sci. U.S.A. 101*, 12783−12788.
(27) Michel, B., Boubakri, H., Baharoglu, Z., LeMasson, M., and Lestini, R. (2007) Recombination proteins and rescue of arrested replication forks. *DNA Repair 6*, 967−980.
(28) Clark, A. J., and Sandler, S. J. (1994) Homologous genetic-recombination: The pieces begin to fall into place. *Crit. Rev. Microbiol. 20*, 125−142.
(29) Koomey, M., Gotschlich, E. C., Robbins, K., Bergstrom, S., and Swanson, J. (1987) Effects of RecA mutations on pilus antigenic variation and phase-transitions in *Neisseria gonorrhoeae*. *Genetics 117*, 391−398.
(30) Sechman, E. V., Kline, K. A., and Seifert, H. S. (2006) Loss of both Holliday junction processing pathways is synthetically lethal in the presence of gonococcal pilin antigenic variation. *Mol. Microbiol. 61*, 185−193.
(31) Cox, M. M. (1998) A broadening view of recombinational DNA repair in bacteria. *Genes Cells 3*, 65−78.
(32) Carroll, J.D., Daly, M. J., and Minton, K. W. (1996) Expression of recA in *Deinococcus radiodurans*. *J. Bacteriol. 178*, 130−135.
(33) Daly, M. J., Ling, O. Y., Fuchs, P., and Minton, K. W. (1994) In-vivo damage and recA-dependent repair of plasmid and chromosomal DNA in the radiaton-resistant bacterium *Deinococcus radiodurans*. *J. Bacteriol. 176*, 3508−3517.
(34) Kim, J. I., and Cox, M. M. (2002) The RecA proteins of *Deinococcus radiodurans* and *Escherichia coli* promote DNA strand exchange via inverse pathways. *Proc. Natl. Acad. Sci. U.S.A. 99*, 7917−7921.
(35) Story, R. M., Weber, I. T., and Steitz, T. A. (1992) The structure of the *Escherichia coli* RecA protein monomer and polymer. *Nature 355*, 318−325.
(36) Chen, Z. C., Yang, H. J., and Pavletich, N. P. (2008) Mechanism of homologous recombination from the RecA-ssDNA/dsDNA structures. *Nature 453*, 483−489.
(37) Wong, O. K., Guthold, M., Erie, D., and Gelles, J. (2000) Multiple conformations of lactose repressor-DNA looped complexes revealed by single molecule techniques. *FASEB J. 14*, 766.
(38) Wong, O. K., Guthold, M., Erie, D. A., and Gelles, J. (2008) Interconvertible lac repressor-DNA loops revealed by single-molecule experiments. *PLoS Biol. 6*, 2028−2042.
(39) Chu, J. F., Chang, T. C., and Li, H. W. (2010) Single-molecule TPM studies on the conversion of human telomeric DNA. *Biophys. J. 98*, 1608−1616.
(40) Schafer, D. A., Gelles, J., Sheetz, M. P., and Landick, R. (1991) Transcription by single molecules of RNA polymerase observed by light microscopy. *Nature 352*, 444−448.
(41) Dohoney, K. M., and Gelles, J. (2001) χ-Sequence recognition and DNA translocation by single RecBCD helicase/nuclease molecules. *Nature 409*, 370−374.
(42) Fan, H. F., and Li, H. W. (2009) Studying RecBCD Helicase Translocation Along χ-DNA Using Tethered Particle Motion with a Stretching Force. *Biophys. J. 96*, 1875−1883.
(43) Kim, J. I., and Cox, M. M. (2002) RecA protein from the extremely radioresistant bacterium *Deinococcus radiodurans*: Expression, purification, and characterization. *J. Bacteriol. 184*, 1649−1660.
(44) Galletto, R., Amitani, I., Baskin, R. J., and Kowalczykowski, S. C. (2006) Direct observation of individual RecA filaments assembling on single DNA molecules. *Nature 443*, 875−878.
(45) Lusetti, S. L., Wood, E. A., Fleming, C. D., Modica, M. J., Korth, J., Abbott, L., Dwyer, D. W., Roca, A. I., Inman, R. B., and Cox, M. M. (2003) C-terminal deletions of the *Escherichia coli* RecA protein: Characterization of in vivo and in vitro effects. *J. Biol. Chem. 278*, 16372−16380.
(46) Story, R. M., and Steitz, T. A. (1992) Structure if the RecA protein-ADP complex. *Nature 355*, 374−376.
(47) Sheridan, S. D., Yu, X., Roth, R., Heuser, J. E., Sehorn, M. G., Sung, P., Egelman, E. H., and Bishop, D. K. (2008) A comparative analysis of Dmc1 and Rad51 nucleoprotein filaments. *Nucleic Acids Res. 36*, 4057−4066.
(48) Yin, H., Landick, R., and Gelles, J. (1994) Tethered particle motion method for studying transcript elongation by a single RNA-polymerase molecule. *Biophys. J. 67*, 2468−2478.
(49) van der Heijden, T., van Noort, J., van Leest, H., Kanaar, R., Wyman, C., Dekker, N., and Dekker, C. (2005) Torque-limited RecA polymerization on dsDNA. *Nucleic Acids Res. 33*, 2099−2105.
(50) Shivashankar, G. V., Feingold, M., Krichevsky, O., and Libchaber, A. (1999) RecA polymerization on double-stranded DNA by using single-molecule manipulation: The role of ATP hydrolysis. *Proc. Natl. Acad. Sci. U.S.A. 96*, 7916−7921.
(51) Pugh, B. F., and Cox, M. M. (1987) Stable binding of RecA protein to duplex DNA-unraveling a paradox. *J. Biol. Chem. 262*, 1326−1336.
(52) Muench, K. A., and Bryant, F. R. (1990) An obligatory pH-mediated isomerization on the Asn-160 RecA protein promoted DNA strand exchange reaction pathway. *J. Biol. Chem. 265*, 11560−11566.
(53) Kowalczykowski, S. C., Clow, J., and Krupp, R. A. (1987) Properties of the duplex DNA-dependent ATPase activity of *Escherichia coli* RecA protein and its role in branch migration. *Proc. Natl. Acad. Sci. U.S.A. 84*, 3127−3131.
(54) Strick, T., Allemand, J. F., Croquette, V., and Bensimon, D. (2000) Twisting and stretching single DNA molecules. *Prog. Biophys. Mol. Biol. 74*, 115−140.
(55) Hilario, J., Amitani, I., Baskin, R. J., and Kowalczykowski, S. C. (2009) Direct imaging of human Rad51 nucleoprotein dynamics on individual DNA molecules. *Proc. Natl. Acad. Sci. U.S.A. 106*, 361−368.
(56) Pugh, B. F., Schutte, B. C., and Cox, M. M. (1989) Extent of duplex DNA underwinding induced by RecA protein binding in the presence of ATP. *J. Mol. Biol. 205*, 487−492.
(57) van der Heijden, T., Seidel, R., Modesti, M., Kanaar, R., Wyman, C., and Dekker, C. (2007) Real-time assembly and disassembly of human RAD51 filaments on individual DNA molecules. *Nucleic Acids Res. 35*, 5646−5657.
(58) Roca, A. I., and Cox, M. M. (1997) RecA protein: Structure, function, and role in recombinational DNA repair. *Prog. Nucleic Acid Res. Mol. Biol. 56*, 129−223.
(59) Benedict, R. C., and Kowalczykowski, S. C. (1988) Increase of the DNA strand assimilation activity of RecA protein by removal of the C-terminus and structure function studies of the resulting protein fragment. *J. Biol. Chem. 263*, 15513−15520.
(60) Tateishi, S., Horii, T., Ogawa, T., and Ogawa, H. (1992) C-Terminal truncated *Escherichia coli* RecA protein RecA5327 has enhanced binding affinities to single stranded and double stranded DNAs. *J. Mol. Biol. 223*, 115−129.
(61) Rajan, R., and Bell, C. E. (2004) Crystal structure of RecA from *Deinococcus radiodurans*: Insights into the structural basis of extreme radioresistance. *J. Mol. Biol. 344*, 951−963.